Chemical Papers (2022) 76:7525–7534
https://doi.org/10.1007/s11696-022-02371-1

ORIGINAL PAPER

Comparative study of adsorption isotherms on activated carbons synthesized from rice husk towards carbon dioxide adsorption

Kishor Palle[1] · Shanthi Vunguturi[1] · K. Subba Rao[2] · Sambhani Naga Gayatri[3] · P. Ramesh Babu[4] · Md. Mustaq Ali[5] · Ramesh Kola[6]

Received: 16 June 2022 / Accepted: 11 July 2022 / Published online: 23 August 2022

Abstract

Rice husk was chemically activated with saturated KOH solution and the activation temperature was varied from 400 to 700 °C to generate activated carbons with different textural characteristics. Activated carbons were investigated for their ability to adsorb CO_2. We selected Langmuir, Freundlich, Sips and Radke-Prausnitz equations to fit the experimental CO_2 adsorption data. In order to determine the effect of using different error standards when calculating isotherm model parameters, an error analysis was conducted. The Radke-Prausnitz model shows the best fit to CO_2 adsorption and calculated adsorption capacity correlates closely with experimental data.

Keywords Rice husk · Activated carbon · Adsorption models · Error analysis · CO_2 adsorption

Introduction

Rice husk is an important biomass resource in South Asia as well as India and China. When compared to other agricultural Bio-wastes rice husk is known for low utilization value as husk and highly utilized as ash that is mostly in the form of silica. Rice husk that is a layer protective for rice grain is that the major by-product obtained from rice processing mill (Nhapi et al. 2011; Zhang et al. 2011).

Global warming has become major concern over the past few years. Increasing greenhouse gas concentrations caused the global average temperature to rise by about 1 °C every year. Among the gases responsible for the greenhouse effect, CO_2 plays the most significant role, since it stays in atmosphere for a significantly longer period of time. By 2020, CO_2 emissions will be over 36 billion tons, up from 2 billion tons in 1900 (Sai Bhargava Reddy et al. 2021). As the amount of harmful CO_2 in atmosphere continues to rise, this is critical for maintaining continued initiatives to minimize worldwide greenhouse gas emissions that cause climatic changes by developing and implementing impressive CO_2 capture methods.

Porous materials are a promising strategy to capture CO_2. In particular, advantages offered by carbon materials such as low desorption temperatures, rapid kinetics and high stability. Carbonaceous materials are very inexpensive if they are made with renewable resources or even waste. So researchers are trying to develop technologies that will enable carbon dioxide to be captured and stored, particularly adsorption technologies are treated as really promising at present (Singh et al. 2017). CO_2 capture is possible with the use of solid adsorbents, which have recently been studied: porous polymers (Sun et al. 2015), zeolites (Nguyen et al. 2016), monoliths (Günay et al. 2007), carbon nanotubes (Elmorsi 2011), carbon nanosheets (Gong et al. 2014), metalloorganic structures (Zhang et al. 2017),

✉ Kishor Palle
drkishorepalle@gmail.com

1 Department of Chemistry, Muffakham Jah College of Engineering and Technology, Hyderabad, Telangana, India

2 Department of Chemistry (H&S), Malla Reddy Engineering College(Autonomous), Main Campus, Secunderabad, Telangana, India

3 Department of Science and Humanities, MLR Institute of Technology, Hyderabad, Telangana, India

4 Department of Physics, Gokaraju Rangaraju Institute of Engineering & Technology, Nizampet Road, Hyderabad, Telangana, India

5 Department of Mathematics (H&S), Malla Reddy Engineering College(Autonomous), Main Campus, Secunderabad, Telangana, India

6 Department of Chemistry, Chaitanya Bharathi Institute of Technology (A), Gandipet, Hyderabad, Telangana, India

activated carbons (Serafifin et al. 2017; Młodzik et al. 2016). In addition to the advantages mentioned above, carbonaceous materials appear to offer several particularly attractive advantages, including a low cost of production, high porosity, high surface area, readily controlled composition, an excellent chemical and thermal stability and high efficiency (Ayawei et al. 2015a; b).

According to equilibrium sorption isotherms, activated carbons adsorption ability and its efficiency can be predicted. An isotherm model with 2, 3, 4, and even 5 parameters are used to describe adsorption process (Elmorsi 2011; Schell et al. 2012a, b). For determining an isotherm of an adsorption and its constant, both experimentation and calculation values are needed. Langmuir, Freundlich, Sips and the Radke-Prausnitz equations were selected among the existing theoretical adsorption models for quantitative comparison of applicability of these models to fit CO_2 adsorption experiments. The amount of gas adsorbed as a function of pressure is defined by the following equations:

Langmuir isotherm

Various models have been developed to describe the adsorption of the gas–solid phase, the Langmuir isotherm being the simplest. A maximum adsorption capacity is also quantified and compared between different sorbents using this method. As described by Langmuir theory, adsorption take place at homogeneous sites in a monolayer of adsorbate. Once a site occupied by adsorbate, no further adsorption happen at that site. As a consequence, capacity of sorbent is limited to adsorb (Elmorsi 2011; Günay et al. 2007). By the following Eq. (1) Langmuir isotherm can be expressed:

$$q = \frac{q_{mL} b_L p}{1 + b_L p} \tag{1}$$

where q_{mL} = maximum adsorption capacity [mmol/g]; b_L = Langmuir constant [bar^{-1}]; p = pressure [bar]; q = adsorbed quantity under p pressure [mmol/g].

Freundlich isotherm

According to Eq. (2), Freundlich's model describes adsorption of different adsorption energies (Ayawei et al. 2015a, b) on heterogeneous surfaces.

$$q = k_F \, p^{n_F} \tag{2}$$

Sips isotherm

Activated carbon is commonly specified using the Sips model, which is typically applied for heterogeneous adsorbents like that (Delavar et al. 2010; Ning et al. 2012). At lower concentrations adsorbate, it becomes the Freundlich model, but Langmuir model is applicable for higher concentrations of adsorbate, it becomes the Langmuir model (Travis and Etnier 1981), then which is represented by Eq. (3):

$$q = \frac{q_{mS} b_S p^{n_S}}{1 + b_S p^{n_{S'}}} \tag{3}$$

where q_{mS} = maximum adsorption capacity [mmol/g]; b_S = Sips constant [bar^{-1}]; n_S = heterogeneity factor.

Radke-Prausnitz isotherm

There are several significant characteristics of Radke-Prausnitz that accomplish an ideal selection for adsorption systems with low concentrations of adsorbate. It becomes a linear isotherm at lower adsorbate concentrations for an adsorption system, a Freundlich isotherm at high concentrations, and a Langmuir isotherm when the $n_{RP} = 0$. Another important property of this isotherm is that it fits a wide range of concentrations of adsorbate. Below is the Radke-Prausnitz Eq. (4) (Radke and Prausnitz 1972):

$$q = \frac{q_{m\mathrm{RP}} b_{\mathrm{RP}} p}{\left(1 + b_{\mathrm{RP}} p\right)^{n_{\mathrm{RP}'}}} \tag{4}$$

where $q_{m\mathrm{RP}}$ = maximum adsorption capacity [mmol/g]; b_{RP} = Radke-Prausnitz constant [bar^{-1}]; n_{RP} = Radke-Prausnitz model exponent.

The fitted isotherm was obtained by using a nonlinear optimization technique. Nonlinear regression can be a useful alternative to linear regression due to the flexibility it provides in fitting curves. As part of nonlinear regression, all the error functions should be diminished. During estimation if the error is small which indicates the prediction is more accurate. SNE(sum of the normalized error) is used to select most suitable set of parameters for all the isotherms based on their smallest error. Complete information of error functions was characterized by Eqs. (5)–(9) and are represented below:

Error function	Equations	References
Sum of the squares of the errors (SSE)	SSE $= \sum_{i=1}^{n} \left(q_{e,\mathrm{calc}} - q_{e,\mathrm{exp}}\right)_i^2$ (5)	Ho (2004)
Hybrid fractional error function (HYBRID)	HYBRID $= \frac{100}{1-p} \sum_{i=1}^{n} \left[\frac{\left(q_{e,\mathrm{calc}} - q_{e,\mathrm{exp}}\right)^2}{q_{e,\mathrm{exp}}} \right]_i$ (6)	Porter et al. (1999)

Error function	Equations	References
Average relative error function (ARE)	ARE $= \frac{100}{1-p}\sum_{i=1}^{n}\left(\frac{q_{e,\mathrm{calc}}-q_{e,\mathrm{exp}}}{q_{e,\mathrm{exp}}}\right)_i$ (7)	Khan et al. (1997)
Marquardt's percent standard deviation (MPSD)	MPSD $= 100\sqrt{\frac{1}{n-p}\sum_{i=1}^{n}\left(\frac{q_{e,\mathrm{calc}}-q_{e,\mathrm{exp}}}{q_{e,\mathrm{exp}}}\right)_i^2}$ (8)	Marquardt (1963)
Sum of the absolute errors function (SAE)	SAE $= \sum_{l=1}^{n}(q_{e,\mathrm{calc}} - q_{e,\mathrm{exp}})_i$ (9)	Ng et al. (2003)

where $q_{e,\mathrm{calc}}$ = calculated adsorption capacity[mmol/g]
$q_{e,\mathrm{exp}}$ = experimentally measured adsorption capacity [mmol/g]

Because the goal of every error function would be to procure a different set of isotherm parameters, these seems to be hard to interpret directly.

It is also possible that another model sum of the normalized errors (SNE) will be recognized as the best based on various error functions. As a result, the error function chosen may have an effect on obtained parameters of the isotherm. The SNE can be used to compare essential parameters. The Sum of normalized errors function (SNE) (Ho 2004):

$$\mathrm{SNE} = \sum_{i=1}^{n}\frac{f_i}{f_{i\max}} \tag{10}$$

The function with the least number SNE and the best-defined empirical results was chosen.

Aim of this work is to investigate CO_2 adsorption on rice husk activated carbons in connection to the investigation of the influence of the isotherm type as well as the model being used determine its parameters by the 2 and 3 parametric models on the calculations while discussing the error functions. The use of KOH as an activator has been the work's novelty. Solid-state carbon materials are presented in the literature. The new method synthesis of activated carbon and impregnation with KOH presented here is much simpler and inexpensive. The use of KOH as an activator was the work's novelty. All of the solid-state carbon sources described in the literature. The new method presented here for preparation of activated carbons and KOH impregnation is much simpler and less expensive.

Materials and methods

Preparation of rice husk activated carbon (RHAC)

Rice husk gathered from rice mill near Telaprolu, Vijayawada, India, was cleaned exhaustively with distilled water to take off adhering soil and dust, and dried at 110 °C overnight. Rice husks were calcined at different temperatures at different atmospheres for 4 h. The temperature was programmed as 10 °C per minute and gas flow maintained at 40 mL per minute (Kishore et al. 2017; Srinivas et al. 2017). Flow chart of activated carbon shown in Fig. 1. Digital images of rice crop, rice husk and its activated carbon were shown in Fig. 2.

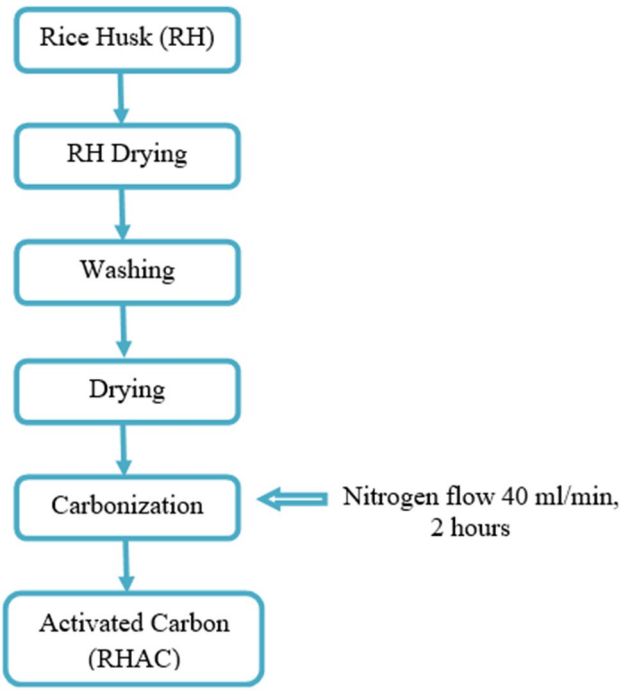

Fig. 1 Flow diagram of preparation of Activated carbon

Chemical activation by using KOH

Synthesized rice husk activated carbons was treated by KOH. Mass ratio of RHAC:KOH was equal to 1:1. Chemical activation of rice husk was carried out with the use of saturated KOH solution. The material was then vigorously mixed till rice husk activate carbon was clearly dissolved in KOH solution and then heated at room temperature about three hours. Following this, the impregnated materials were dried at 200 °C about 20 h in laboratory dryer. After the impregnation carbonization is carried out for synthesized activated carbons. In horizontal electric furnace tubular reactor was placed to carry out the process of physical activation between the range of 400–700 °C temperature, after this increase the temperature at a rate of 10 °C per minute to a predetermined value.The procedure was carried out in a nitrogen-carbon dioxide environment (flow rate of 18 dm^3/h, carbon dioxide flow rate of 5 dm^3/h). In all of the trials, the activation process parameters such as duration, N_2-CO_2 flow rate, and heating rate of furnace were the same. They were

Fig. 2 Digital images of rice crop, rice husk and activated carbon

thought, based on numerous prior studies, the optimal settings results assuring highest improvement of surface area of examined activated carbon materials.

To achieve a neutral reaction, activated carbons comprising with KOH or K_2CO_3 was washed with deionized water. These activated carbons were soaked with a 1 mol/dm^3 HCl solution and left for 20 h after evaporation. Carbons were then washed with deionized water till the chloride ions being completely removed. The product was dried for 16 h at 110 °C. Synthesized activated carbons labelled as: RHAC-KOH-400, RHAC-KOH-500,RHAC-KOH-600, RHAC-KOH-700, where: RHAC is rice husk activated carbon, KOH is an activating agent and 400, 500, 600, 700 are activation temperatures. A pore size analyzer and sorption surface area (ASAP 2460, Micrometrics, Novcross, USA) instrument is used to analyse Nitrogen adsorption at – 196 °C for all activated carbon samples. For eliminating impurities of activated carbons, adsorption tests were proceeded by 12 h of heating at 250 °C at 1°/min heating rate under decreased pressure due to continual running of pump. The following characteristics defining the porous structure were acquired using N_2 sorption isotherms:

- Surface area (SBET) calculated using the BET equation and a partial pressure in the range of $p/p0 = 0.05–0.2$. This range was determined separately for each material in order to achieve linearity of function (11).
- Nitrogen vapours maximal adsorption at $p/p0 = 0.99$ is used to estimate total pore volume (Vp,N_2)

$$f\left(\frac{p}{p_0}\right) = \frac{1}{W\left(\frac{p}{p_0} - 1\right)} \tag{11}$$

where W = mass of gas adsorbed at a relative pressure p/p_0; p = nitrogen pressure; $p_0 = 1.01$ bar;

The DFT approach was used to analyse pores variety of mesopores and micropores (Vmic,N_2) utilizing N_2 analysis at – 196 °C temperature (density functional theory).

The Nitrogen adsorption isotherm at – 196 °C provides information regarding the micropore structure, partially macropores and mesopores. The CO_2 adsorption activities were performed using ASAP at 0 °C temperature and 1 bar pressure. To regulate the temperature of the experiment, the investigated were placed in a thermostat. The activated carbons were out-gassed for 12 h prior to the CO_2 adsorption tests at a temperature of 250 °C.

Results and discussion

Figure 3 depicts the findings of the N_2 adsorption–desorption isotherms of investigated activated carbons.The isotherms revealed that microporous materials exhibit high

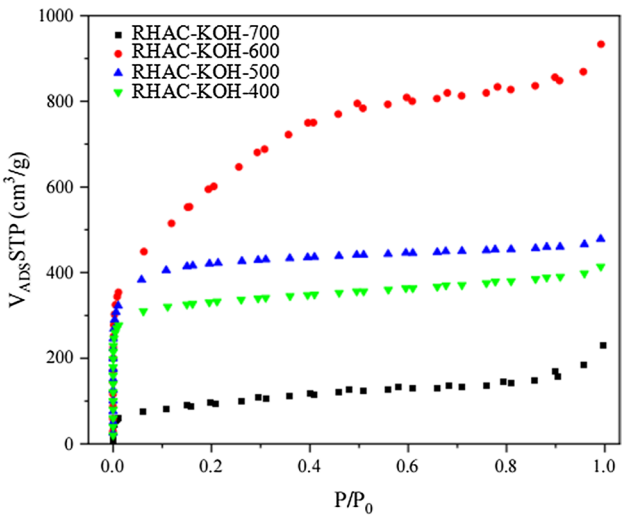

Fig. 3 Activated carbons nitrogen adsorption–desorption isotherms

N_2 adsorption at low relative pressure. It indicates larger micropore volume with narrow pore size distribution. The N_2 adsorption determined at – 196 °C temperature rose remarkably in all carbon materials as the activation temperature raised during the heat treatments, the carbon activated at maximum temperature (800 °C) exhibit lowest N_2 adsorption is the only one exception.

The N_2 adsorption isotherms belong to Type I for low pressure and Type IV for middle and higher ranges, according to the International Union of Pure and Applied Chemistry (IUPAC). The presence of a clearly developed hysteresis loop, which would be associated to capillary condensation in mesopores region, is a distinguishing Type IV isotherm characteristics. Type IV hysteresis loop is formed by isotherms. In mesopores, capillary condensation takes place between relative pressure range $p/p0 = 0.45–1$, indicating presence of mesopores in all four samples.

More detailed information about the structure of the adsorption over investigated samples may be obtained by analyzing the pore size distribution. An investigation of distribution of pore size for activated carbon materials based on N_2 adsorption was undertaken to examine correlation between pore size of analyzed carbon materials and of the activation process temperature. The pore distribution depicted in Fig. 4 demonstrates that all the activated carbon materials, additionally rather extensively developed microporosity, have advanced mesoporosity.

The selected approach offers information about porosity of pores with in ranging between 0.34 and 302 nm, according to adsorbate applied. Although, only holes up to 5 nm are shown in Fig. 4 since no bigger pores were found in the studied activated carbons.

Table 1 Activated carbons surface area, pore volume and micropore volume taken from nitrogen adsorption isotherms at – 196 °C

Sample	S_{BET} [m^2/g]	$V_{p,N2}$ [cm^3/g]	$V_{mic,N2}$ [cm^3/g]
RHAC-KOH-400	248	0.63	0.39
RHAC-KOH-500	576	0.72	0.52
RHAC-KOH-600	1074	1.42	0.45
RHAC-KOH-700	124	0.35	0.06

Table 1 shows the textural characteristics of all samples. In case of samples RHAC-KOH-400, RHAC-KOH-500, RHAC-KOH-600, with increasing activation temperature, greater surface areas and pore volumes were achieved. Moreover, as shown in Table 1, the trend differs for sample RHAC-KOH-700. High surface area (1074 m^2/g) achieved for RHAC-KOH-600 sample. The RHAC-KOH-500 carbon has shown highest micropore volume of 0.52 cm^3/g with excellent microporosity.

Activated carbon was tested at 0℃ temperature under 1 bar pressure and adsorption of CO_2 was measured. In Fig. 5, we show the experimental CO_2 adsorption capacity at 0 °C.

A decrease in carbonization temperature was found to increase CO_2 adsorption capacity at 0 °C.

It is surprising that these results conflict with literature reports (Wang and Yang 2012) which show that efficiency of CO_2 adsorption increases by increasing specific surface area as well as volume of total pores. It follows that for synthesized activated carbons, pores whose diameters are in the range of 0.3 to 0.6 nm are the most important, while pores that are larger play an almost insignificant role. The results

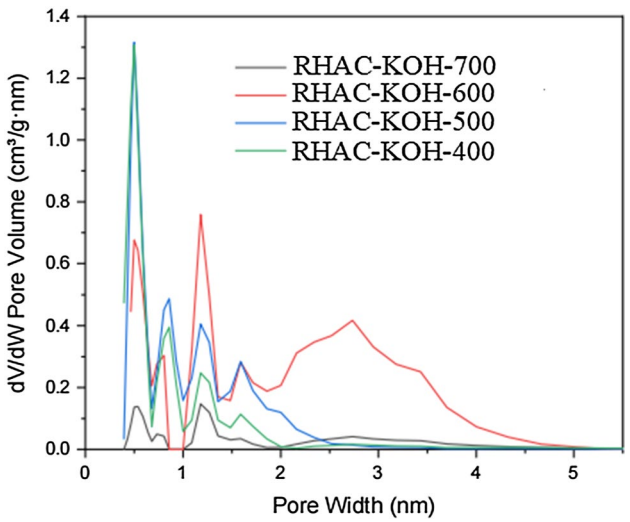

Fig. 4 Distribution of pores size of activated carbon materials

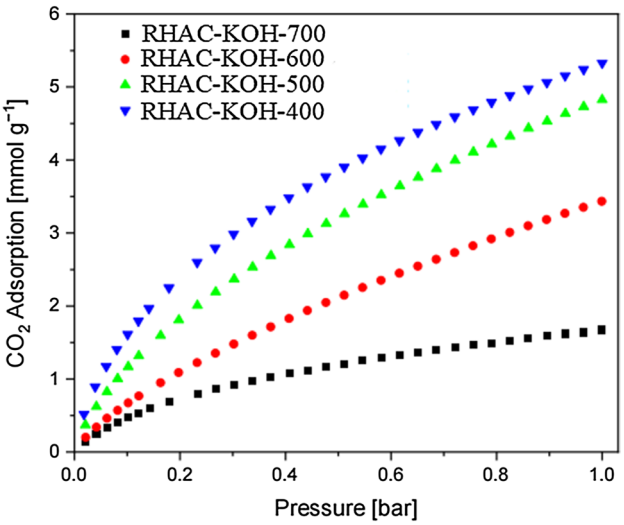

Fig. 5 Measured isotherms of adsorption of CO_2 at 0 °C

Table 2 Langmuir CO_2 adsorption of various activated carbons at 1 bar and 0 °C

Material	CO_2 adsorption at 0 °C [mmol/g]	References
Organic framework polymers	2.9	Li et al. (2013)
Activated carbon xerogels	4.9	Martin-Jimeno et al. (2015)
Mg and N-doped mesoporous carbon	3.7	Liu et al. (2021)
Waste wool-derived N-doped hierarchical porous carbon	3.7	Li et al. (2018)
Polyaniline-graphene oxides	3.2	Rodriguez-Garcia et al. (2019)
KOH activated carbon derived from rice husk	5.3	This work

Table 3 Langmuir isotherms constants with error analysis

	SSE	HYBRID	ARE	MPSD	SAE
RHAC-KOH-400					
q_{mL}	7.2707	6.7818	6.6419	6.1657	7.5580
b_L	2.4183	2.8826	2.9746	3.6483	2.1633
SSE	0.505	0.6586	0.7666	1.4430	0.5884
HYBRID	1.1769	0.9676	0.9984	1.3673	1.5786
ARE	5.9061	5.4549	5.4176	5.9606	6.4050
MPSD	11.1292	9.0957	8.9495	7.9138	12.8738
SAE	3.39919	3.9596	4.1155	5.5469	3.1862
SNE	3.4954	**3.3413**	3.4467	4.4115	3.9822
RHAC-KOH-500					
q_{mL}	.0398	7.2929	7.0237	6.3559	8.2289
b_L	1.39 8	l.6943	1.7979	2.2240	1.3194
SSE	0.2922	0.4024	0.5183	1.1479	0.3200
HYBRID	0.8823	0.7123	0.7452	1.0937	].()465
ARE	5.8638	5.4440	5.2:687	5.8189	6.1 97
MPSD	11.0699	8.9443	8.5690	7.5538	12.0371
SAE	2:.5697	3.1291	3.3528	4.6078	2.4829
SNE	3.5118	**3.3383**	3.4842	4.5691	3.8010
RHAC-KOH-600					
q_{mL}	7.2701	6.5517	6.2432	5.3984	7.7763
b_L	2.4183	1.0075	l.0685	1.3850	0.7605
SSE	0.5058	0.1395	0.1987	0.4368	0.1048
HYBRID	1.1769	0.3865	0.4222	0.6498	0.5752
ARE	5.9061	5.2092	5.1408	5.5799	6.0437
MPSD	11.1292	8.7370	8.5614	7.2350	11.6905
SAE	3.3992	1.8368	l.9745	2.9106	1.4299
SNE	4.9292	**2.7539**	2.9155	3.8141	3.1167
RHAC-KOH-700					
q_{mL}	2.3634	2.2 177	2.1264	2.0454	2.4152
b_L	2.1749	2.5319	2.7403	3.0590	2.0372
SSE	0.0354	0.0463	0.0669	0.0955	0.0392
HYBRID	0.2405	0.1916	0.2128	0.2700	0.3046
ARE	5.0117	4.5123	4.3913	4.6334	5.3820
MPSD	8.8630	6.8759	6.3129	5.7975	10.0703
SAE	0.9143	1.0524	1.1685	1.3988	0.8799
SNE	3.6249	**3.3866**	3.6769	4.3230	4.0390

Standard uncertainties of all constants are equal to 0.001, uncertainties of all errors equal to 0.0001 (0.5 level of confidence)

Table 4 Freundlich isotherms constants with error analysis

	SSE	HYBRID	ARE	MPSD	SAE
RHAC-KOH-400					
q	5.4205	5.4856	5.5150	5.5975	5.3964
b_F	1.5139	1.5354	0.5367	0.5603	0.5012
SSE	0.1401	0.1980	0.22:11	0.4431	0.1625
HYBRID	0.3874	0.2846	0.2923	0.4152	0.5647
ARE	3.2034	2.8662	2.8350	3.2776	3.6642
MPSD	7.2039	5.1631	5.1589	4.2316	8.8241
SAE	1.7629	2.1561	2.1921	3.0892	1.6738
SNE	3.2636	3.0160	3.0845	4.1093	3.9085
RHAC-KOH-500					
q	4.8747	4.9154	4.9327	4.9916	4.8676
b_F	0.6134	1.6293	0.6314	0.6487	0.6054
SSE	0.0351	0.0542	0.0638	0.1471	0.04 14
HYBRID	0.1387	0.09 6	0.1008	0.1565	0.1980
ARE	2.1842	1.9252	1.9129	2.2214	2.4765
MPSD	5.1089	3.6259	3.5209	2.8951	6.1199
SAE	0.8572	1.1171	1.1772	1.7416	0.7960
SNE	3.1485	2.8783	2.9663	4.1604	3.7383
RHAC-KOH-600					
q	3.4494	3.4629	3.4653	3.4932	3.44 6
b_F	0.7105	0.7184	0.7183	0.7294	0.7080
SSE	0.0025	0.0044	0.0045	0.0161	0.0027
HYBRID	0.0198	0.014 1	0.0142	0.0254	0.0243
ARE	1.0365	0.9412	0.9334	1.1573	1.1344
MPSD	2.6721	1.9611	1.9862	1.5462	2.9536
SAE	0.2122	0.3164	0.3168	0.5735	0.2036
SNE	3.1073	2.8550	2.8730	4.5235	3.4631
RHAC-KOH-700					
q	1.7039	1.7311	1.7350	l.7808	1.6913
b_F	0.5361	0.5655	0.5627	0.6016	0.5148
SSE	0.0199	0.0299	0.0293	0.0754	0.0257
HYBRID	0.2135	0.1537	0.1561	0.2358	0.3477
ARE	4.2889	3.8856	3.8502	4.5703	5.1219
MPSD	10.3752	7.3861	7.7001	5.9423	13.3000
SAE	0.6473	0.8396	0.8150	1.2886	0.5973
SNE	2.9977	2.8043	2.8004	4.0172	3.8045

Standard uncertainties of all constants are equal to 0.001, uncertainties of all errors equal to 0.0001 (0.5 level of confidence)

Table 5 Sips isotherms constants with error analysis

	SSE	HYBRID	ARE	MPSD	SAE
RHAC-KOH-400					
q_{mS}	14.5122	13.5991	13.6306	12.6177	13.6362
bs	0.5774	0.6389	0.6348	0.7201	0.6347
n_S	0.6698	0.6835	0.6811	0.6985	0.6823
SSE	0.0021	0.0032	0.0040	0.0084	0.0039
HYBRID	0.0079	0.0055	0.0063	0.0084	0.0062
ARE	0.3765	0.3752	0.3598	0.4799	0.3625
MPSD	1.1333	0.7660	0.8467	0.6191	0.7971
SAE	0.1846	0.2621	0.2434	0.4270	0.2415
SNE	3.4052	**3.1082**	3.2932	4.5463	3.2227
RHAC-KOH-500					
q_{mS}	22.6789	19.8826	19.9379	17.2029	17.4800
bs	0.2698	0.3190	0.3172	0.3856	0.3777
n_S	0.7046	0.7193	0.7165	0.7353	0.7366
SSE	0.0016	0.0025	0.0029	0.0073	0.0061
HYBRID	0.0076	0.0051	0.0059	0.0083	0.0091
ARE	0.4527	0.4383	0.4209	0.5216	0.5614
MPSD	1.2981	0.8558	0.9880	0.6795	0.7877
SAE	0.1736	0.2488	0.2427	0.3972	0.3692
SNE	3.2912	**2.9670**	3.1687	4.3638	4.3763
RHAC-KOH-600					
q_{mS}	42.7761	32.7762	32.7525	24.6378	24.7621
bs	0.0873	0.1168	0.1168	0.1609	0.1602
n_S	0.7457	0.7567	0.7550	0.7697	0.7728
SSE	0.0004	0.0006	0.0008	0.0022:	0.0018
HYBRID	0.0031	0.0021	0.0023	0.0036	0.0043
ARE	0.3799	0.3564	0.3413	0.4385	0.4809
MPSD	1.1134	0.7421	0.8305	0.5790	0.7074
SAE	0.0834	0.1195	0.1201	0.2177	0.2004
SNE	3.0586	**2.7163**	2.9021	4.2867	4.3704
RHAC-KOH-700					
q_{mS}	4.0852	3.6207	3.6222	3.2118	3.9718
bs	0.6867	0.8426	0.8377	1.0460	0.7162
n_S	0.7222	0.7558	0.7507	0.7898	0.7249
SSE	0.0011	0.0017	0.0019	0.0044	0.0013
HYBRID	0.0130	0.0086	0.0095	0.0131	0.0135
ARE	0.9887	0.9161	0.8855	1.0281	0.%17
MPSD	2.6725	1.6678	1.8912	1.2971	2.7228
SAE	0.1519	0.2034	0.1936	0.2998	0.1507
SNE	3.6710	**3.2133**	3.3430	4.4471	3.7447

Standard uncertainties of all constants are equal to 0.001, uncertainties of all errors equal to 0.0001 (0.5 level of confidence)

of carbon dioxide adsorption on activated carbon materials generated from many carbon sources are summarized in Table 2.

According to IUPAC classification, all isotherms correspond to microporous adsorbents, which are characteristic of type I. The adsorption isotherms for CO_2 were derived from experimental data in each model.

As shown in Tables 3, 4, 5, and 6, based on SNE there are sets of parameters and error functions of CO_2 adsorption isotherm. The SNE was compared and therefore, the isotherm constants that fit the measured data the best were obtained. As shown in Tables 3, 4, 5, and 6, bolded letters denote the minimum SNE value for activated carbon of each isotherm, and underlined letters denote lowest SNE value and the set of optimal parameters of activated carbons of all the isotherms.

Table 3 shows the results of fitting parameters to the Langmuir model.

By utilizing different error functions, nonlinear regression was used to estimate the constants. The constants q_{mL} and b_L values have very high similarity. The Langmuir isotherm is not a useful model for the adsorption of CO_2 over all the activated carbon samples. Based on the SNE values, HYBRID is the best overall Langmuir fit across all 4 activated carbon materials.

In Table 4, we present the Freundlich isotherm constants and error functions.

The ARE give the best Freundlich fit for RHAC-KOH-700, and HYBRID for RHAC-KOH-400, RHAC-KOH-500, RHAC-KOH-600 according to SNE. In spite of this, the best Freundlich fit cannot be accepted.

The Set of parameters for fitting Sips model are represented in Table 5.

Based on the SNE, the HYBRID was the best fit for SIPs.

Table 6 represents isotherms constants and error functions of Radke-Prausnitz model.

Specifically, the SNE stipulated MPSD for RHAC-KOH-600, ARE for RHAC-KOH-700, and HYBRID for RHAC-KOH-400 & RHAC-KOH-500 provides the best Radke-Prausnitz fit. With respect to error functions, the three constants qmRP, bRP, and nRP are comparable. In all error functions only qmRP, bRP, nRP constants are approximate. The SNE is lowest for RHAC-KOH-400, RHAC-KOH-700 in all the established models. A rational approximation for optimal set of parameters is given by Radke-Prausnitz

Table 6 Radke-Prausnitz isotherms constants with error analysis

	SSE	HYBRID	ARE	MPSD	SAE
RHAC-KOH-400					
q_{mRP}	6.0801	6.0346	6.0345	6.0045	6.1359
b_{RP}	7.1453	7.7204	7.7204	8.2684	6.5972
n_{RP}	0.6237	0.6114	0.6107	0.5990	0.6353
SSE	0.0018	0.0027	0.0029	0.0059	0.0027
HYBRID	0.0057	0.0038	0.0039	0.0055	0.012
ARE	0.3647	0.3350	0.3324	0.3670	0.4673
MPSD	0.9164	0.5601	0.5688	0.4408	1.4428
SAE	0.1993	0.2577	0.2611	0.3621	0.1 96
SNE	2.7259	**2.5733**	2.6215	3.5170	3.9580
RHAC-KOH-500					
q_{mRP}	5.7020	5.6944	5.6881	5.6828	5.7173
b_{RP}	5.5569	5.5968	5.6404	5.6899	5.4427
n_{RP}	0.5016	0.5008	0.4998	0.4981	0.5042
SSE	0.0002	0.0001	0.0002	0.0002	0.0001
HYBRID	0.0002	0.0002	0.0002	0.0002	0.0003
ARE	0.0753	0.0656	0.0619	0.0651	0.0900
MPSD	0.1246	0.1044	0.0929	0.0871	0.2103
SAE	0.0511	0.0470	0.0491	0.0579	0.0456
SNE	2.9617	**2.5525**	2.7331	3.5854	3.8452
RHAC-KOH-600					
q_{mRP}	4.0263	3.6978	3.7420	4.1119	4.0787
b_{RP}	5.8348	13.9867	11.7225	5.0523	5.3481
n_{RP}	0.3585	0.3127	0.3203	0.3718	0.3647
SSE	0.0001	0.0014	0.0009	0.0002	0.0001
HYBRID	0.0003	0.0058	0.0048	0.0004	0.0003
ARE	0.1371	0.5852	0.5081	0.1379	0.1231
MPSD	0.3185	1.3273	1.2821	0.1701	0.2063
SAE	0.0444	0.1795	0.1349	0.0708	0.0473
SNE	1.8140	4.0187	3.0246	**0.2076**	0.4890
RHAC-KOH-700					
q_{mRP}	2.0027	1.8197	2.0092	2.0170	1.9999
b_{RP}	5.0158	12.7788	4.8565	4.7483	5.0536
n_{RP}	0.6512	0.5146	0.6605	0.6660	0.6503
SSE	0.0001	0.0133	0.0001	0.0002	0.0001
HYBRID	0.0005	0.0746	0.0005	0.0005	0.0006
ARE	0.2146	2.6605	0.1799	0.1885	0.2209
MPSD	0.4830	4.9792	0.2943	0.2309	0.5463
SAE	0.0402	0.5515	0.0480	0.0594	0.0388
SNE	0.2633	5.0000	**0.2306**	0.2450	0.2773

Standard uncertainties of all constants are equal to 0.001, uncertainties of all errors equal to 0.0001 (0.5 level of confidence)

equation. Figure 6. represents theoretical and experimental data of Radke-Prausnitz isotherms.

For empirical data analysis, the Radke-Prausnitz model is recommended. Based on Fig. 4, a similar conclusion can be reached. It seems that irrespective of the error function, the experimental isotherm suits rather well with the Radke-Prausnitz equation model.

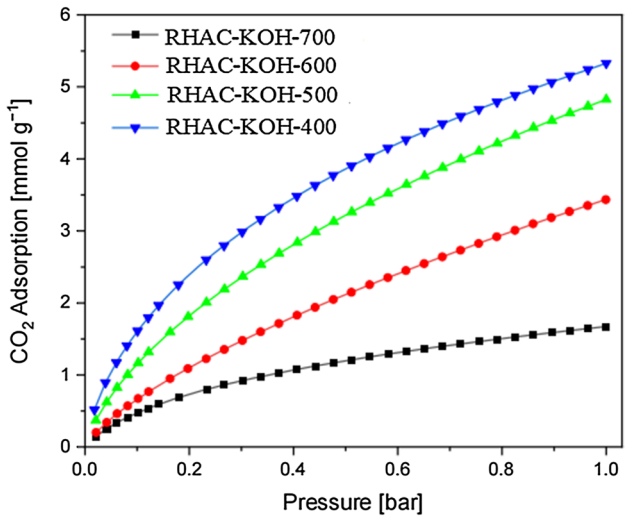

Fig. 6 Carbon dioxide adsorption isotherms at 0 °C. Based on lowest SNE, empirical results are expressed by symbols, lines were prevailed by Radke-Prausnitz model

Conclusions

The CO_2 adsorption findings at 0 °C on four activated carbons produced by using rice husk and treated with KOH solution suggest that these activated carbons may be useful for improving CO_2 adsorption. The measured specific surface area and pore volume is as large as 1074 m^2g^{-1} and 1.42 cm^3g^{-1} respectively, related to the activated carbon designated as RHAC-KOH-600. Interestingly, reduction in the carbonization temperature significantly increased the CO_2 adsorption ability at temperatures 0 °C. At 0 °C temperature and 1 bar pressure, activated carbon labelled as RHAC-KOH-400 shown highest CO_2 adsorption as 5.3 $mmolg^{-1}$. The equilibrium adsorption findings were calculated and analyzed using 4 distinct isotherms and 5 different optimization and error functions. The error function was compared using the sum of normalized errors, and the optimum isotherm equation was determined. The best estimation is provided by the Radke-Prausnitz model, because it is significant model for actual data.

Acknowledgements The authors acknowledge financial support of this work from department of Chemistry, MJCET, which is operated and managed by Sultan-ul-Uloom Education Society and also grateful to the Hon. Secretary, SUES and Advisor-cum director, and other colleagues of Chemistry department, MJCET, Hyderabad for their encouragement and support in completing this work successfully.

Data availability The data of the current study are available from the corresponding author on reasonable request.

Declarations

Conflict of interest On behalf of all the authors, the corresponding author states that there is no conflict of interest.

References

Ayawei N, Angaye SS, Wankasi D, Dikio ED (2015a) Synthesis, characterization and application of Mg/Al layered double hydroxide for the degradation of congo red in aqueous solution. Open J Phys Chem 5:56–70. https://doi.org/10.4236/ojpc.2015.53007

Ayawei N, Ekubo AT, Wankasi D, Dikio ED (2015b) Adsorption of congo red by Ni/Al—CO3: equilibrium, thermodynamic and kinetic studies. Orient J Chem 31:1307–1318. https://doi.org/10.13005/ojc/310307

Delavar M, Ghoreyshi AA, Jahanshahi M, Irannejad M (2010) Experimental evaluation of methane adsorption on granular activated carbon (GAC) and determination of model isotherm. Eng Technol 62:47–50

Elmorsi TM (2011) Equilibrium isotherms and kinetic studies of removal of methylene blue dye by adsorption onto miswak leaves as a natural adsorbent. J Environ Prot Ecol 2:817–827. https://doi.org/10.4236/jep.2011.26093

Gong J, Michalkiewicz B, Chen X, Mijowska E, Liu J, Jiang Z, Wen X, Tang T (2014) Sustainable conversion of mixed plastics into porous carbon nanosheets with high performances in uptake of carbon dioxide and storage of hydrogen. ACS Sustain Chem Eng 2:2837–2844. https://doi.org/10.1021/sc500603h

Günay A, Arslankaya E, Tosun I (2007) Lead removal from aqueous solution by natural and pretreated clinoptilolite: adsorption equilibrium and kinetics. J Hazard Mater 146:362–371. https://doi.org/10.1016/j.jhazmat.2006.12.034

Ho YS (2004) Selection of optimum sorption isotherm. Carbon 42:2115–2116. https://doi.org/10.1016/j.carbon.2004.03.019

Khan AR, Al-Bahri T, Al-Haddas A (1997) Adsorption of phenol based organic pollutants on activated carbon from multicomponent dilute aqueous solution. Water Res 31:2101–2112. https://doi.org/10.1016/S0043-1354(97)00043-2

Kishore P, Srinivas BN, Rao KS, Turaka AK, Prasad NBL (2017) Carbon dioxide adsorption studies of rice husk ash prepared in different atmospheres. Int J Recent Innov Eng Res 2(7):26–31. https://doi.org/10.15680/IJIRSET.2016.0608043

Li T, Sullivan JE, Rosi NL (2013) Design and preparation of a core–shell metal–organic framework for selective CO2 capture. J Am Chem Soc 135:9984–9987. https://doi.org/10.1021/ja403008j

Li Y, Xu R, Wang X, Wang B, Cao J, Yang J, Wei J (2018) Waste wool derived nitrogen-doped hierarchical porous carbon for selective CO_2 capture. RSC Adv 35:19818–19826. https://doi.org/10.1039/C8RA02701C

Liu B, Shi R, Ma X, Chen R, Zhou K, Xu X, Sheng P, Zeng Z, Li L (2021) High yield nitrogen-doped carbon monolith with rich ultramicropores prepared by in-situ activation for high performance of selective CO2 capture. Carbon 181:270–279. https://doi.org/10.1016/j.carbon.2021.05.029

Marquardt DW (1963) An algorithm for least squares estimation of non-linear parameters. J Soc Ind Appl Math 11:431–441

Martin-Jimeno FJ, Suarez-Garcia F, Paredes JI, Martinez-Alonso A (2015) Activated carbon xerogels with a cellular morphology derived from hydrothermally carbonized glucose-graphene oxide hybrids and their performance towards CO_2 and dye adsorption. Carbon 81:137–147. https://doi.org/10.1016/j.carbon.2014.09.042

Młodzik J, Sre'nscek-Nazzal J, Narkiewicz U, Morawski AW, Wróbel RJ, Michalkiewicz B (2016) Activated carbons from molasses as CO_2 sorbents. Acta Phys Pol A 129:402–404. https://doi.org/10.1007/978-3-319-16901-9_29

Ng JCY, Cheung WH, McKay G (2003) Equlibrium studies for the sorption of lead from effluents using chitosan. Chemosphere 52:1021–1030. https://doi.org/10.1016/S0045-6535(03)00223-6

Nguyen TH, Gong H, Lee SS, Bae TH (2016) Amine-appended hierarchical Ca-A zeolite for enhancing CO_2/CH_4 selectivity

of mixed-matrix membranes. Chem Phys Chem 17:3165–3169. https://doi.org/10.1002/cphc.201600561

Nhapi I, Banadda N, Murenzi R, Sekomo C, Wali U (2011) Removal of heavy metals from industrial waste water using rice husks. Open Environ Eng J 4:170–180. https://doi.org/10.2174/1874829501104010170

Ning P, Li F, Yi H, Tang X, Peng J, Li Y, He D, Deng H (2012) Adsorption equilibrium of methane and carbon dioxide on microwave-activated carbon. Sep Purif Technol 98:321–326. https://doi.org/10.1016/j.seppur.2012.07.001

Porter F, McKay G, Choy KH (1999) The prediction of sorption from a binary mixture of acidic dyes using single and mixed isotherms variants of the ideal adsorbed solute theory. Chem Eng Sci 54:5863–5885. https://doi.org/10.1016/S0009-2509(99)00178-5

Radke CJ, Prausnitz JM (1972) Adsorption of organic solutions from dilute aqueous solution on activated carbon. Ind Eng Chem Fundam 11:445–451. https://doi.org/10.1021/i160044a003

Rodriguez-Garcia S, Santiago R, Lopez-Diaz D, Merchan MD, Velazquez MM, Fierro JLG, Palomar J (2019) Role of the structure of graphene oxide sheets on the CO_2 adsorption properties of nanocomposites based on graphene oxide and polyaniline or Fe_3O_4-nanoparticles. ACS Sustain Chem Eng 7:12464–12473. https://doi.org/10.1021/acssuschemeng.9b02035

Sai Bhargava Reddy M, Ponnamma D, Sadasivuni KK, Kumar B, Abdullah AM (2021) Carbon dioxide adsorption based on porous materials. RSC Adv 11:12658–12681. https://doi.org/10.1039/D0RA10902A

Schell J, Casas N, Blom R, Spjelkavik AL, Andersen A, Hafifizovic Cafka J, Mazzotti M (2012a) MCM-41, MOF and UiO-67/MCM-41 adsorpbents for pre-combustion CO_2 capture by PSA: adsorption equilibria. Adsorption 18:213–227. https://doi.org/10.1007/s10450-012-9395-1

Schell J, Casas N, Pini R, Mazzotti M (2012b) Pure and binary adsorption of CO2, H2, N2 on activated carbons. Adsorption 18:49–65. https://doi.org/10.1007/s10450-011-9382-y

Serafifin J, Narkiewicz U, Morawski AW, Wróbel RJ, Michalkiewicz B (2017) Highly microporous activated carbons from biomass for CO_2 capture and effective micropores at different conditions. J CO2 Util 18:73–79. https://doi.org/10.1016/j.jcou.2017.01.006

Singh G, Kim IY, Lakhi KS, Srivastava P, Naidu R, Vinu AB (2017) Single step synthesis of activated bio-carbons with a high surface area and their excellent CO_2 adsorption capacity. Carbon 116:448–455. https://doi.org/10.1016/j.carbon.2017.02.015

Srinivas BN, Kishore P, Rao KS, Kumar TA (2017) Preparation of surface modified activated carbons from rice husk and CO_2 adsorption studies. IOSR J Appl Chem 10:54–60

Sun LB, Kang YH, Shi YQ, Jiang Y, Liu XQ (2015) Highly selective capture of the greenhouse gas CO_2 in polymers. ACS Sustain Chem Eng 3:3077–3085. https://doi.org/10.1021/acssuschemeng.5b00544

Travis CC, Etnier EL (1981) A survey of sorption relationships for reactive solutes in soil. J Environ Qual 10:8–17. https://doi.org/10.2134/jeq1981.00472425001000010002x

Wang L, Yang RT (2012) Significantly increased CO_2 adsorption performance of nanostructured templated carbon by tuning surface area and nitrogen doping. J Phys Chem C 116:1099–1106. https://doi.org/10.1021/jp2100446

Zhang J, Fu H, Lv X, Tang J, Xu X (2011) Removal of Cu (II) from aqueous solution using the rice husk carbons prepared by the physical activation process. Biomass Bioenergy 35(1):464–472. https://doi.org/10.1016/j.biombioe.2010.09.002

Zhang K, Qiao Z, Jiang J (2017) Molecular design of zirconium tetrazolate metalorganic frameworks for CO_2 capture. Cryst Growth Des 17:543–549. https://doi.org/10.1021/acs.cgd.6b01405